PAPER

New approach for fabricating hybrid-structured metal mesh films for flexible transparent electrodes by the combination of electrospinning and metal deposition

To cite this article: Jin Woo Huh *et al* 2016 *Nanotechnology* **27** 475302

IOP Publishing Nanotechnology
Nanotechnology 27 (2016) 475302 (7pp) doi:10.1088/0957-4484/27/47/475302

New approach for fabricating hybrid-structured metal mesh films for flexible transparent electrodes by the combination of electrospinning and metal deposition

Jin Woo Huh, Dong Kyu Lee, Hwan-Jin Jeon[1] and Chi Won Ahn[1]

Department of Nano-Structured Materials Research, Korea National Nanofab Center, Daejeon 305-701, Korea

E-mail: hjjeon@nnfc.re.kr and cwahn@nnfc.re.kr

Received 14 July 2016, revised 20 September 2016
Accepted for publication 30 September 2016
Published 25 October 2016

Abstract

In this study, hybrid-structured metal mesh (HMM) films as potential flexible transparent electrodes, composed of aligned micro-sized metal fibers integrated into random network of metal nanofibers, were fabricated by the combination of electrospinning and metal deposition. These naturally fiber-bridged HMMs, with a gold layer thickness of 85 nm, exhibited a high transmittance of around 90% and a sheet resistance of approximately 10 $\Omega\,sq^{-1}$, as well as favorable mechanical stability under bending stress. These results demonstrate that the approach employed herein is a simple, highly efficient, and facile process for fabricating, uniform, interconnected fiber networks with potential for producing high-performance flexible transparent electrodes.

S Online supplementary data available from stacks.iop.org/NANO/27/475302/mmedia

Keywords: hybrid structure, metal mesh, aligned microfiber, flexible transparent electrode, electrospinning

(Some figures may appear in colour only in the online journal)

1. Introduction

It is imperative to fabricate nano- and micro-sized transparent electrodes with high flexibility for use as components in various future optoelectronic devices, such as paper-like displays [1, 2], touch screen [3], flexible light-emitting diodes [4], photovoltaic cells [5, 6], and smart windows [7]. Although conductive metal oxides such as indium tin oxide (ITO) and fluorine tin oxides are typically used, these metal oxides are brittle, as well as they tend to crack when substrates are bent or stretched. These drawbacks have prompted research into the use of materials such as conducting polymers [4, 8–12], carbon nanotubes [13–16], graphene [3, 17–20] and metal nanowire grids [21–25] for use in flexible transparent electrodes. Particularly, metal nanowire grids are considered to be promising candidates, attributed to their excellent reproducibility of a uniform metal frame, which achieves optimal electrical conductivity and transmittance.

Recently, Guo *et al* [21] have fabricated nanoscale metal grids by nanoimprinting, which could potentially be a practical solution for fabricating semitransparent metal electrodes for organic light emitting diodes applications. However, this process is complex and incurs high cost, attributed to the use of top–down processes, such as metallization and lift-off, for achieving the necessary nanoscale pattern. Peuman *et al* [22] have fabricated solution-processed flexible transparent electrodes, composed of random metal nanowire meshes. Despite the advantages of a solution-based process, it is not suitable for synthesizing continuous long nanowires exhibiting high

[1] Authors to whom any correspondence should be addressed.

theoretical electric conductivity in accordance to the percolation theory [26, 27].

On the other hand, electrospinning has received considerable attention for the effective fabrication of high-performance transparent electrodes, attributed to its simplicity, cost-effectiveness, and scalability for the production of uniform, continuous, ultra-long electric channels composed of various materials, including organics and inorganics [28–32]. Several researchers have attempted to employ electrospinning for obtaining metal micro or nanofibers for applications in flexible or stretchable transparent electrodes [33–37]. In a study performed by Cui *et al* a new type of highly flexible transparent electrode, composed of metallic (Ag) nanotrough networks [36] with metal mesoscale (ranging from 1 to 5 um) fibers integrated into these synthesized Ag nanowire networks [37], was fabricated by electrospinning as well as nanowire film and metal deposition. These transparent electrodes exhibit highly enhanced optoelectronic performance, attributed to their uniform and interconnected networks caused by the even distribution of the polymer nanofiber template achieved by electrospinning. This in turn leads to reduced contact junction resistance and improved percolation parameters. In addition, the integration of metal mesoscale wires into Ag nanowire networks results in the significant improvement of local conductance and resistance-transmittance performance, attributed to a large cross-sectional area for electron transport via mesoscale metal wires, which can effectively reduce power loss even at high transmittance.

In this study, hybrid-structured metal mesh (HMM) films, composed of the combination of structures with aligned micro-sized metal fiber arrays and random networks of nano-sized metal fibers, were fabricated by a new, highly efficient process based on electrospinning for use as flexible transparent electrodes. This developed technique is based on the generation of different-sized electrospun polymer fibers by controlling the parameters of electrospinning, as well as transfer to metal fibers via metal deposition. The technique for fabricating conducting nanostructures for flexible transparent electrodes exhibits the following advantages: (i) this method can generate well-woven conducting metal nanofibers with varying diameters of 100–300 nm, which are bridged between micro-sized fibers with diameters of 1–3 um over a large area. (ii) Such fiber webs can be fabricated as freestanding films without any substrates and subsequently transferred very easily to all kinds of substrates. (iii) Different sizes and complex structures can be prepared by simply changing the conditions of electrospinning. (iv) This approach allows for the fabrication of freestanding transparent flexible thin films with various conducting materials, which can be utilized to deposition.

For demonstrating this novel approach, a gold HMM thin film was fabricated for use in flexible transparent electrodes. The resulting HMM film exhibited a high transmittance of around 90% at 550 nm, a sheet resistance of around $10\,\Omega\,\mathrm{sq}^{-1}$, and a bending radius of 5 mm (with a bending strain (ε) of 2%). These results are superior to those of commercial flexible ITO films (ITO/Polyethylene terephthalate (PET) substrate). This simple, rapid, and versatile fabrication technique demonstrates immense potential for the production of high-performance flexible transparent electrodes and their future applications.

2. Experimental

2.1. Fabrication of hybrid-structured PVP nanomesh.

Mesh structures with micro/nano-sized organic fibers were prepared by electrospinning (Nano NC Co., Korea, ESN-HV30B) with a polyvinylpyrrolidone (PVP, $\mathrm{Mw} = 1.3 \times 10^6\,\mathrm{g\,mol}^{-1}$, Acros) solution. The process is based on electrospun ultra-long polymer fiber templates. The PVP solution was produced by dissolving PVP powder in ethanol (99.5%, Sigma-Aldrich), and solutions with 4–8 wt% and 14–17 wt% of PVP were used for fabricating nano-sized and micro-sized polymer fibers, respectively. The dispersed PVP solution was transferred into a metal-tipped syringe (0.50 mm inner diameter, 21G). The parameters utilized were an electric field on the order of 5–6 kV, and the distance between the needle tip and grounded collector was 13 cm, along with a pump rate of 0.2–0.4 ml h^{-1}. A 3 cm long square aluminum frame (width 3 cm) was used as the substrate for gathering the electrospun fibers. Polymer nanoscale fibers with diameters of approximately 100–300 nm were randomly networked using a circular collector. And then, the randomly networked nanofibers were transferred onto an aluminum frame with free-standing form. Next, the aligned electrospun polymer microscale fibers with diameters of 1–3 um were collected on a two-parallel edge collector, which has a 3 cm gap between edges. The aligned microscale fibers were scooped up with the frame which the freestanding nanofiber networks were previously formed on, and were then assembled on the freestanding nanofiber networks.

2.2. Transfer to the HMM

For fabricating the HMM, a 10 nm thick Cr layer (adhesion layer) and a 85 nm thick gold layer were deposited on the freestanding mesh structured films with mixed nano- and micro-sized polymer fibers within the aluminum frame by electron-beam evaporation at a base pressure of approximately 10^{-6} Torr. For removing the preformed polymer nanofibers, ethanol was used. The metal meshes in the frame were deposited on substrates, such as glass and plastic films, after placing several drops of ethanol on the substrate. Once ethanol evaporated from the substrates, the frame was then lifted and removed.

2.3. Characterization

The surface features and morphology of the mesh-structured fiber webs were characterized by scanning electron microscopy (Sirion FE-SEM, FEI) and optical microscopy (Leica Microsystems). Sheet resistance was characterized by a four-point probe system (Cascade Microtech, Inc.) using a source-measure unit (4200-SCS, Keithley). Transmittance was recorded on a UV–Visible/NIR spectrophotometer (Lambda

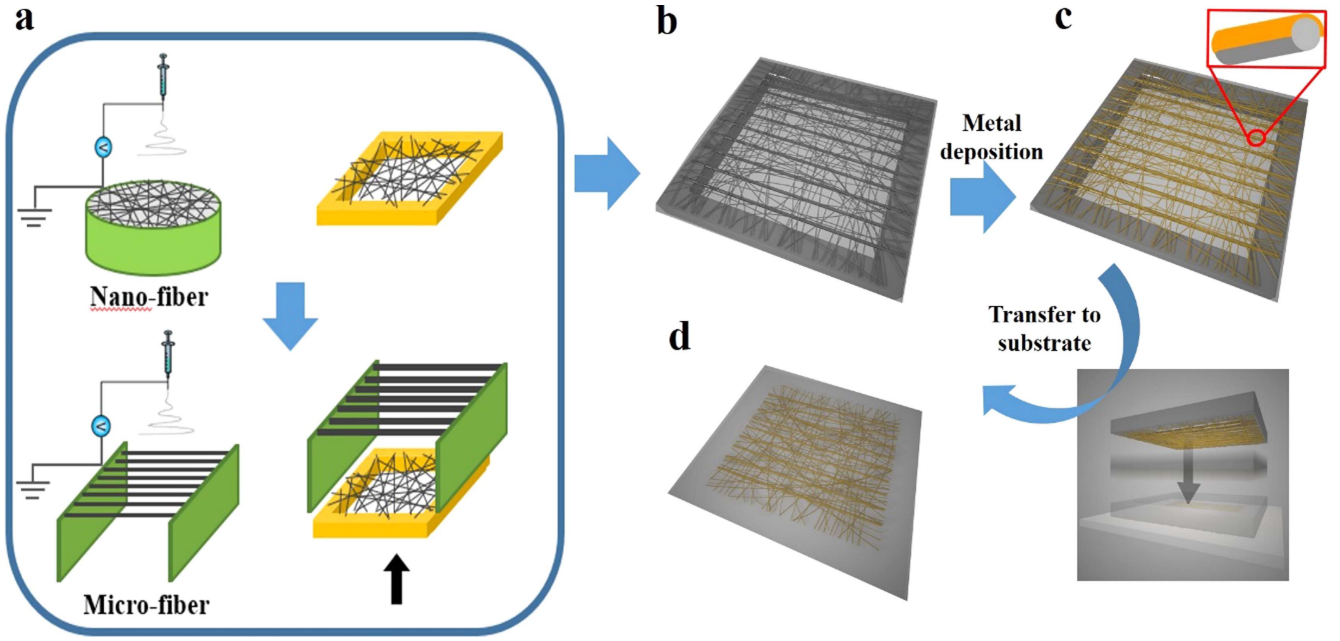

Figure 1. Schematic for the fabrication of the HMM transparent electrode film with mixed metal micro- and nano-fibers. (a), (b) Hybrid-structured polymer mesh structures. (c) Metal mesh film produced via metal deposition. (d) Transfer of metal mesh structures on substrates.

1050, PerkinElmer). Mechanical stability was analyzed using a bending test system. The system consisted of a two-contact interface serving to induce compressive stress to the sample, where one interface was fixed and immobile, while the other was allowed to move laterally using a motion controller (T-LSR075D, Zaber).

3. Results and discussion

Figure 1 shows the schematic for the fabrication of an HMM transparent electrode film by electrospinning and metal deposition. First, nano-sized polymer fiber networks were created as a framework by using a circular collector during electrospinning (figure 1(a), top image). Next, the aligned micro-sized polymer fiber arrays were fabricated with high regularity and order by using a two-parallel edge collector for electrospinning (figure 1(a), bottom image). The aligned micro-sized fibers were then assembled on the nanofiber networks for affording hybrid mesh-structured nanofiber webs (figure 1(b)). Following assembly, layers of metals, such as gold and copper, were deposited on a single side of the polymer fiber templates via either e-beam or thermal deposition (figure 1(c)). These metal-deposited fiber webs were then transferred to the desired substrates (figure 1(d)). In this final process, several drops of ethanol were dropped on the substrate for removing the polymer fibers. After the removal of polymer fibers, only the metal fiber web structures were retained on the desired substrates (figure 1(d)). Notably, the HMM structures could successfully be transferred on substrates through the physical contacts between the free-standing HMM structures and substrates during transfer process.

Figure 2 shows the SEM and optical images of the fabricated electrospun polymer fiber templates and HMMs. Random networks of interconnected polymer nanofibers were observed (figure 2(a)). The polymer microfibers were observed to be aligned uniaxially with a gap of ~100 um, which is the optimum gap space for obtaining high transmittance (>90%) at a low sheet resistance according to previous simulation results [37] (figure 2(b)). Polymer templates composed of nanofiber networks integrated with arrayed microfibers were then successfully achieved, as shown in figure 2(c). Both the synthesized nano- and micro-fibers exhibited ultra-long length (figures 2(a)–(c)). In addition, various diameters, ranging from several hundreds of nanometers to several micrometers, were controlled well, and the diameter scales of those differed by one order of magnitude (figure 2(d)). Figure 2(e) shows HMMs after the deposition of gold and subsequent transfer on substrates. Notably, metal fibers, composed of a semi-cylindrical metal shell layer covering the lower part of the polymer fibers, were naturally interconnected at both microfiber–nanofiber junctions (figure 2(f)) and nanofiber–nanofiber junctions (figure 2(g)), ensuring a low contact resistance between the metal fibers. As shown in figures 2(f) and (g), metal fibers were spontaneously linked to each other (more images were shown in supplementary figure S1), attributed to the electrospun polymer templates comprising well-woven fiber webs.

For demonstrating the excellent performance of our HMM films, the electrical and optical properties of the films were analyzed. The optoelectrical effect related to the incorporation of the aligned metal microfiber arrays into metal nanofiber networks was investigated. Figure 3 shows the transmittance of these nanofiber networks with and without metal microfiber arrays. The transmittance values of the metal nanofiber networks with and without microfiber arrays at

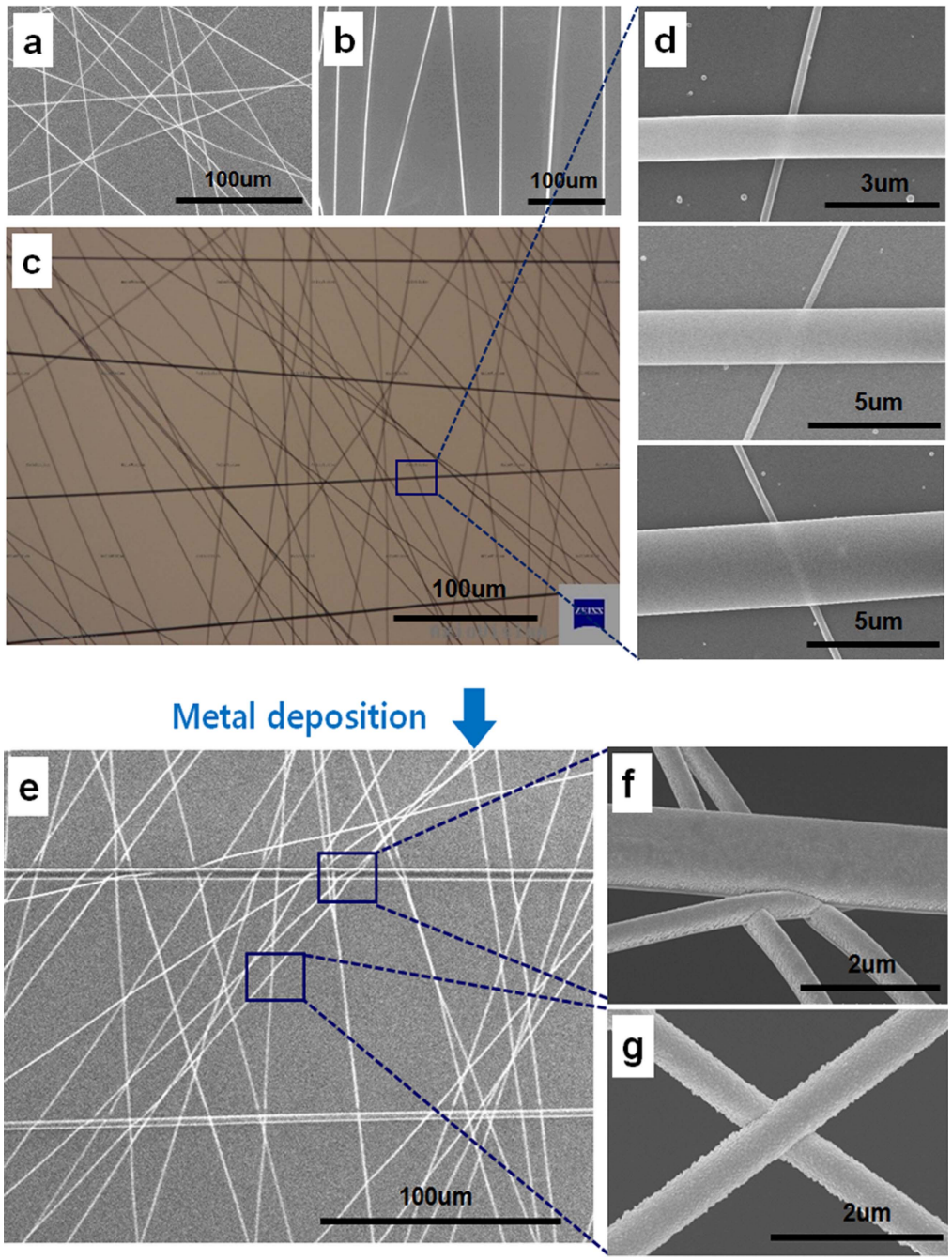

Figure 2. HMM films with electrospun nano- and micro-fiber templates before gold deposition (a)–(d) and after gold deposition (e)–(g). SEM images of (a) randomly networked polymer nanoscale fibers and (b) uniaxially aligned polymer microscale fibers. (c) Optical image of the polymer templates assembled with aligned microfibers and underlying nanofiber networks. (d) High-magnification SEM images of the polymer microfiber and nanofiber with microfiber diameters of 1, 2, and 3 um and a nanofiber diameter of 200 nm. SEM images of (e) gold HMMs fabricated on polymer templates, (f) micro- and nano-fiber junctions, and (g) nano- and nano-fiber junctions after the deposition of gold.

550 nm were 87% and 91%, respectively, comparable to that of conventional ITO in both cases. The sheet resistance values of the networks containing microfiber arrays and only the nanofiber network were $7.8\,\Omega\,\mathrm{sq}^{-1}$ and $125.6\,\Omega\,\mathrm{sq}^{-1}$, respectively. This result implies that the introduction of metal microfiber arrays into metal nanofiber networks leads to the marked enhancement of electrical conductance without a significant decrease in transmittance. Moreover, the transmittance of the metal microfiber arrays integrated into the metal nanofiber webs also exhibited an excellent flat spectrum over the entire visible range, which is highly desirable for several optoelectronic devices.

Figures 4(a) and (b) show the transmittance and sheet resistance of the gold HMMs, where polymer templates, incorporating varying micro-polymer fiber diameters of approximately 1, 2, and 3 um into networks of nano-polymer

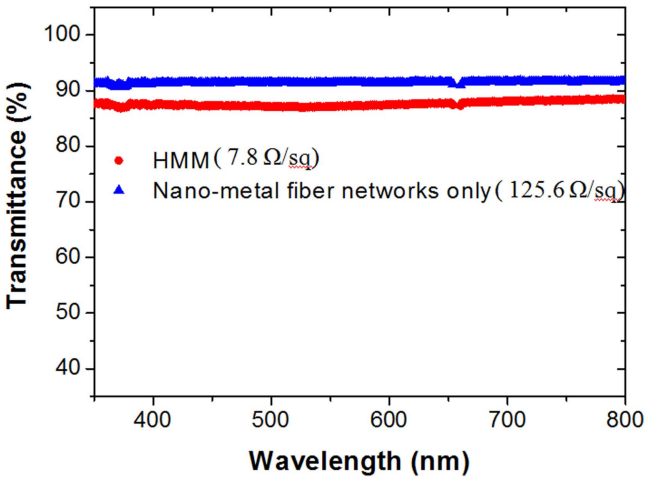

Figure 3. Transmittance spectra of 85 thick gold HMMs and nanofiber metal networks on glass substrates (polymer templates with polymer fiber diameters of 3 um (micro-fiber) and 300 nm (nano-fiber), as well as network films of only nano-polymer fibers with a diameter of 300 nm, were used for fabricating HMMs here.).

fibers with diameter of 200 nm, as shown in figure 2(d), were employed. As can be observed in figure 4(a), transmittance spectra were flat over the entire optical range and remained high (greater than 87%) though the transmittance slightly decreased with increasing diameter; in the inset images, the metal mesh films were transferred on glass and PES plastic substrates and were highly transparent (as evidenced from the clearly observed institutional logo from the top image). In figures 4(a) and (b), the transmittance values of metal microfibers with diameters of 1, 2, and 3 um were 91%, 89%, and 87%, and their corresponding sheet resistance values were 24.8, 9.9, and 7.6 $\Omega\,\mathrm{sq}^{-1}$ at 550 nm, respectively. This optoelectronic properties of the gold HMM networks are well described by percolation theory. The relation between transmittance T and sheet resistance R_s in percolation network, is depicted by [26, 27]

$$T = \left[1 + \frac{1}{\Pi}\left(\frac{Z_0}{R_s}\right)^{\frac{1}{(n+1)}}\right]^{-2},$$

where n is the percolation exponent, Z_0 the impedance of free space (377 Ω) and $\prod$ the percolative figure-of-merit. This formula shows that high $\prod$ and low n values are desired for achieving low R_s coupled with high T and suggests that the percolative regime can be identified as a straight line on a log–log plot of $T^{-1/2} - 1$ versus R_s/Z_0. Percolation parameters, n and $\prod$, can be derived by the interception and slope of fitting line in the log–log plot. Here, the optoelectronic data of gold HMM films were fitted using the formula as shown in figure 4(c), which confirms the performance of HMM films follows percolation theory. From the fitting line, n and $\prod$ for the HMMs were found to be 2.0 and 52, respectively. Referring to previous reports [27], the n value of 2.0 is within the bounds expected for true percolation exponents, and the value of $\prod$ follows the orders: Au HMM (52) > Ag nanowires (32) > sing-walled nanotube (18) > graphene (3.5). This implies that the percolation parameters of the HMM networks are competitive to the value of other nanostructured thin films, which proves the high performance of the HMM films due to good interconnection and uniformity of the HMM networks. Also, the optoelectronic properties of the copper HMM networks are presented in supporting information figure S2. On the other hand, sheet resistance was observed to decrease with increasing metal microfiber diameter, attributed to the enhancement of the conduction properties of the sheet caused by the increased cross-sectional area of the conduction path related to the increased diameter. From the results shown in figure 4(b), a micro-fiber diameter of 2 um is suitable for achieving high transmittance and low sheet resistance in HMM films.

For evaluating the flexibility of our HMMs as flexible transparent electrodes, the HMM structures were transferred onto a 200 um thick polyethersulfone (PES) substrate with an area of 2.5 cm × 2.5 cm. The mechanical stability of the HMM films with various bending radii of 5, 10, and 20 mm in the bent state was examined by *in situ* resistance measurements. At each value of bending radius, all samples were bent, and the resistance was monitored in conjunction with bending. Figure 4(d) shows the relative increase in resistance ($\Delta R/R_0$, ratio of the resistance increase at a specific bending radius to the initial resistance at zero strain) and bending strain (ε) with respect to bending radius for the HMM films ($\varepsilon = d/(2R)$, where d is the substrate thickness, and R is the bending radius). In figure 4(d), no obvious decrease in conductance up to a bending radius of 5 mm was observed, corresponding to a bending strain (ε) of 2%. The mechanical stability of the hybrid metal mesh films was also compared with that of commercialized flexible ITO films after bending cycles (figure 5).The flexibility of the nano metal networks was examined and presented in supporting information figure S3. Considering the result of figure 4(d), a bending radius of 5 mm was chosen for comparison. As shown in figure 5, the resistance of the HMMs exhibited marginal change even after 1000 bending cycles. Meanwhile, the ITO film exhibited increased resistance as well as drastic decrease in conductance even at a low number of bending cycles (greater han 50 times). This result can be attributed to the favorable bonding at the junctions between metal nano- and nano-fibers and between metal nano- and micro-fibers, caused by the naturally interconnected electrospun polymer fiber templates, which serve as the skeletons of the HMM structure. These results indicate that the HMM film has potential use as flexible transparent electrodes.

4. Conclusions

In this study, HMMs films composed of aligned metal microfibers and randomly networks of metal nanofibers were fabricated by a new, highly efficient process. These HMMs demonstrated potential for use as flexible transparent electrodes. Metal micro- and nanofibers, serving as the components of the HMM, were prepared by electrospinning and metal deposition. Size tuning and fiber interconnection of the

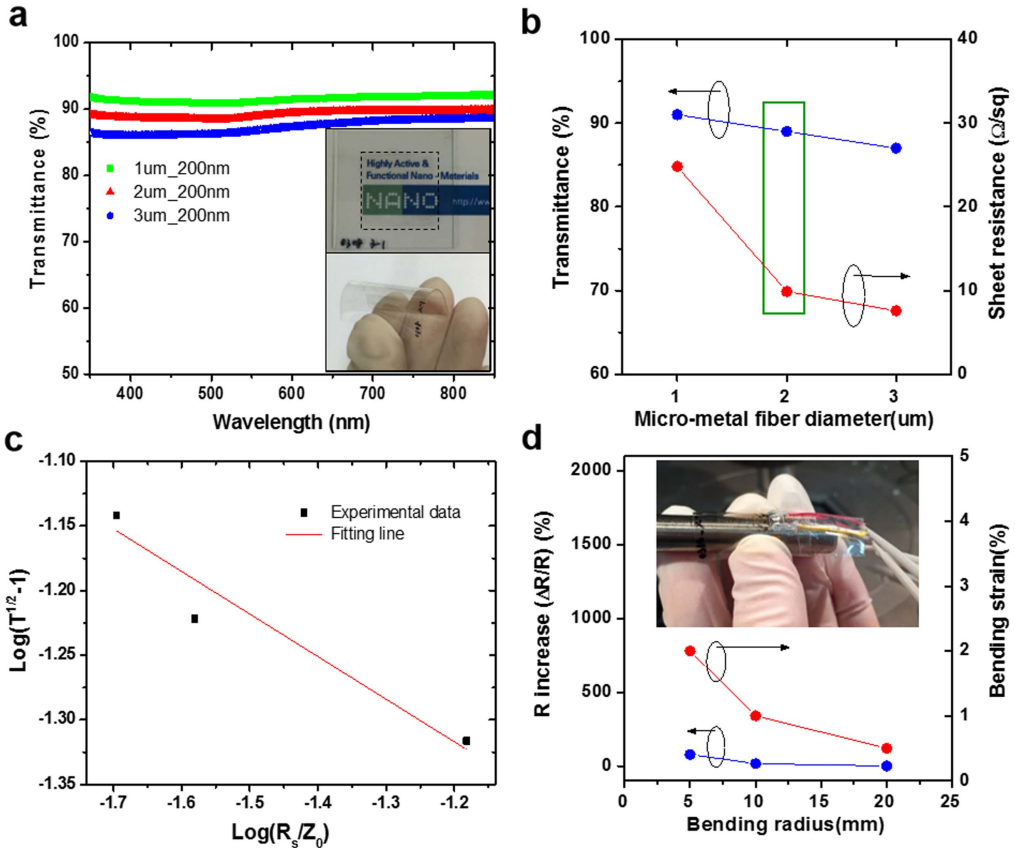

Figure 4. (a) Transmittance spectra (inset: actual photographs of the HMM films on glass (above) and PES (below) substrates) (b) transmittance at 550 nm and sheet resistance of HMM films with gold thickness of 85 nm as a function of metal micro-fiber diameter (c) fitting line of R_s–T performance of HMM films in percolative regime (d) *in situ* relative increase in the resistance and bending strain of HMM film on the PES substrate as a function of the bending radius (inset: photograph of a HMM film prepared and bent for *in situ* resistance measurement at a bending radius of 5 mm).

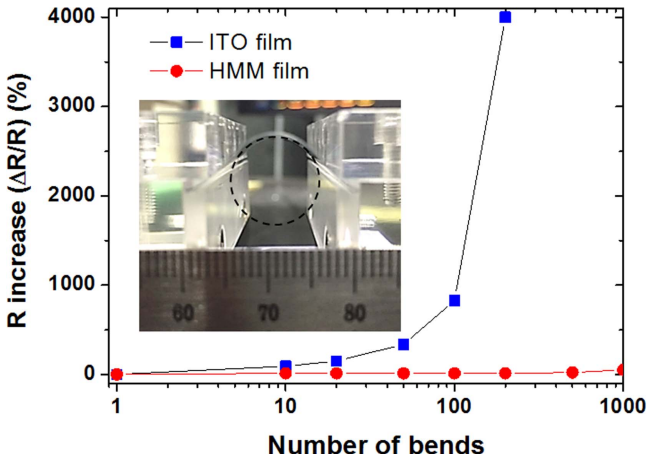

Figure 5. Relative increase in the resistance of the ITO film on the PET substrate and the HMM film on the PES substrate as a function of the number of cycles of repeated bending to a radius of 5 mm (inset: photograph of a bent HMM film with a bending radius of 5 mm using the bending machine).

HMMs were easily achieved using electrospun polymer fiber templates. The transmittance of the 85 nm thick Au layered HMMs with microfiber diameters of 2 um and nanofiber diameters of 200 nm was approximately 90% at 10 $\Omega\,sq^{-1}$. The mechanical flexibility of the HMM films under bending stresses was also favorable, demonstrating properties suitable for use in flexible optoelectronic device applications. These results demonstrate the process proposed here is suitable for fabricating readily uniform, interlinked networks composed of nano- and micro-fibers. Based on these results, it is expected that the HMM films and the described process for their fabrication demonstrate the potential for their use in flexible transparent electrodes.

Acknowledgments

This research was supported financially by a grant from the Leading Foreign Research Institutes Recruitment Program (NRF-2015K1A4A3047100), (NRF-2015M3A7B7046618) and (NRF-2015M3A7B6027973), Funded by the Ministry of Science, ICT, and Future Planning, Korea (MSIP).

References

[1] Bai P F, Hayes R A, Jin L L, Shui L L, Yi Z C, Wang L, Zhang X and Zhou G F 2014 Review of paper-like display technologies *Prog. Electromagn. Res.* **147** 95–116

[2] Kwon S H, Lee S G, Cho W K, Ryu B G and Song M B 2006 Flexible paper-like diaply using charged polymer particles *SID Symp. Digest of Technical Papers* vol 37, pp 1838–40

[3] Bae S, Kim H, Lee Y, Xu X, Park J-S, Zheng Y, Balakrishnan J, Lei T, Kim H R and Song Y I 2010 Roll-to-roll production of 30 inch graphene films for transparent electrodes *Nat. Nanotechnol.* **5** 574–8

[4] Gustafsson G, Cao Y, Treacy G M, Klavetter F, Colaneri N and Heeger A J 1992 Flexible light-emitting diodes made from soluble conducting polymers *Nature* **357** 477–9

[5] Gordon R G 2000 Criteria for choosing transparent conductors *MRS Bull.* **25** 52–7

[6] Jeon H-J, Kim K H, Baek Y–K, Kim D W and Jung H–T 2010 New top–down approach for fabricating high-aspect-ratio complex nanostructures with 10nm scale features *Nano Lett.* **10** 3604–10

[7] Deb S K, Lee S-H, Tracy C E, Pitts J R, Gregg B A and Branz H M 2001 Stand-alone photovoltaic-powered electrochromic smart window *Electrochim. Acta* **46** 2125–30

[8] Sirringhaus H, Kawase T, Friend R H, Shimoda T, Inbasekaran M, Wu W and Woo E P 2000 High-resolution inkjet printing of all-polymer transistor circuits *Science* **290** 2123–6

[9] Kushto G P, Kim W and Kafafi Z H 2005 Flexible organic photovoltaics using conducting polymer electrodes *Appl. Phys. Lett.* **86** 093502

[10] Fehse K, Walzer K, Leo K, Lovenich W and Elschner A 2007 Highly conductive polymer anodes as replacements for inorganic materials in high-efficiency organic light-emitting diodes *Adv. Mater.* **19** 441–4

[11] Huh J W, Kim Y M, Park Y W, Choi J H, Lee J W, Lee J W, Yang J W, Ju S H, Paek K K and Ju B K 2008 Characteristics of organic light-emitting diodes with conducting polymer anodes on plastic substrates *J. Appl. Phys.* **103** 044502

[12] Vosgueritchian M, Lipomi D J and Bao Z 2012 Highly conductive and transparent PEDOT:PSS films with a fluorosurfactant for stretchable and flexible transparent electrodes *Adv. Funct. Mater.* **22** 421–8

[13] Wu Z *et al* 2004 Transparent, conductive carbon nanotube films *Science* **305** 1273–6

[14] Zhang D, Ryu K, Liu X, Polikarpov E, Ly J, Tompson M E and Zhou C 2006 Transparent, conductive, and flexible carbon nanotube films and their application in organic light-emitting diodes *Nano Lett.* **6** 1880–6

[15] Li J, Hu L, Wang L, Zhou Y, Gruner G and Marks T J 2006 Organic light-emitting diodes having carbon nanotube anodes *Nano Lett.* **6** 2472–7

[16] Hecht D S, Hu L and Irvin G 2011 Emerging transparent electrodes based on thin films of carbon nanotubes, graphene, and metallic nanostructures *Adv. Mater.* **23** 1482–513

[17] Li X, Zhang G, Bai X, Sun X, Wang X, Wang E and Dai H 2008 Highly conducting graphene sheets and Langmuir–Blodgett films *Nat. Nanotechnol.* **3** 538–42

[18] Eda G, Fanchini G and Chhowalla M 2008 Large-area ultrathin films of reduced graphene oxide as a transparent and flexible electronic material *Nat. Nanotechnol.* **3** 270–4

[19] Wang X, Zhi L J and Mullen K 2008 Transparent, conductive graphene electrodes for dye-sensitized solar cells *Nano Lett.* **8** 323–7

[20] Kim K S, Zhao Y, Jang H, Lee S Y, Kim J M, Kim K S, Ahn J, Kim P, Choi J and Hong B H 2009 Large-scale pattern growth of graphene films for stretchable transparent electrodes *Nature* **457** 706–10

[21] Kang M-G and Guo L J 2007 Nanoimprinted semitransparent metal electrodes and their application in organic light-emitting diodes *Adv. Mater.* **19** 1391–6

[22] Lee J-Y, Connor S T, Cui Y and Peumans P 2008 Solution-processed metal nanowire mesh transparent electrodes *Nano Lett.* **8** 689–92

[23] Ahn S H and Guo L J 2010 Spontaneous formation of periodic nanostructures by localized dynamic wrinkling *Nano Lett.* **10** 4228–34

[24] Jeon H–J, Jeong H S, Kim Y H, Jung W–B, Kim J Y and Jung H–T 2014 Fabrication of 10 nm-scale complex 3D nanopatterns with multiple shapes and components by secondary sputtering phenomenon *ACS Nano* **8** 1204–12

[25] Jeon H–J, Kim T Y, Jung W–B, Jeong H–S, Kim Y H, Shin D O, Jung S J, Shin J, Kim S O and Jung H–T 2016 Complex high aspect ratio metal nanostructures by secondary sputtering phenomenon combined with block copolymer self-assembly *Adv. Mater.* **28** 8439–45

[26] De S and Coleman J N 2011 The effects of percolation in nanostructured transparent conductors *Mater. Res. Soc. Bull.* **36** 774–81

[27] De S, King P J, Lyons P E, Khan U and Coleman J N 2010 Size effects and the problem with percolation in nanostructured transparent conductors *ACS Nano* **4** 7064–72

[28] Li D and Xia Y N 2004 Electrospinning of nanofibers: reinventing the wheel? *Adv. Mater.* **16** 1151–70

[29] Greiner A and Wendorff J H 2007 Electrospinning: a fascinating method for the preparation of ultrathin fibers *Angew. Chem., Int. Ed. Engl.* **46** 5670–703

[30] Bognitzki M, Becker M, Graeser M, Massa W, Wendorff J H, Schaper A, Weber D, Beyer A, Golzhauser A and Greiner A 2006 Preparation of sub-micrometer copper fibers via electrospinning *Adv. Mater.* **18** 2384–6

[31] Li D and Xia Y N 2003 Fabrication of titania nanofibers by electrospinning *Nano Lett.* **3** 555–60

[32] Wu H, Zhang R, Liu X X, Lin D D and Pan W 2007 Electrospinning of Fe, Co, and Ni nanofibers: synthesis, assembly, and magnetic properties *Chem. Mater.* **19** 3506–11

[33] Hsu P C, Wu H, Carney T J, McDowell M T, Yang Y, Garnett E C, Li M, Hu L and Cui Y 2012 Passivation coating on electrospun copper nanofibers for stable transparent electrodes *ACS Nano* **6** 5150–6

[34] Li H, Pan W, Zhang W, Huang S and Wu H 2013 TiN nanofibers: a new material with high conductivity and transmittance for transparent conductive electrodes *Adv. Funct. Mater.* **23** 209–14

[35] Soltanian S, Rahmanian R, Gholamkhass B, Kiasari N M, Ko F and Servati P 2013 Highly stretchable, sparse, metallized nanofiber webs as thin, transferrable transparent conductors *Adv. Energy Mater.* **3** 1332–7

[36] Wu H, Kong D, Ruan Z, Hsu P-C, Wang S, Yu Z, Carney T J, Hu L, Fan S and Cui Y 2013 Transparent electrode based on a metal nanotrough network *Nat. Nanotechnol.* **8** 421–5

[37] Hsu P-C, Wang S, Wu, Narasimhan V K, Kong D, Lee H R and Cui Y 2013 Performance enhancement of metal nanowire transparent conducting electrodes by mesoscale metal wires *Nat. Commun.* **4** 1–7